Sensors and Materials, Vol. 29, No. 10 (2017) 1391–1398
MYU Tokyo

S & M 1431

X-ray-Induced Luminescence of SnO–SrO–B_2O_3 Glasses Prepared under Different Preparation Conditions

Hirokazu Masai,* Takayuki Yanagida,[1] Go Okada,[1]
Akitoshi Koreeda,[2] and Takahiro Ohkubo[3]

National Institute of Advanced Industrial Science and Technology,
1-8-31 Midorigaoka, Ikeda, Osaka 563-8577, Japan
[1]Nara Institute of Science and Technology, 8916-5 Takayama, Ikoma, Nara 630-0192, Japan
[2]Department of Physical Science, Ritsumeikan University, 1-1-1 Nojihigashi, Kusatsu, Shiga 525-8577, Japan
[3]Graduate School & Faculty of Engineering, Chiba University, 1-33 Yayoi, Chiba 263-8522, Japan

(Received February 2, 2017; accepted July 28, 2017)

Keywords: glass, luminescence, Sn^{2+}, proration condition, structure

Since the physical properties and network structure of glass depend on the quenching process from the supercooled liquid state, it is expected that the luminescence of doped activators will also be dominated by the preparation condition. Here, we have investigated the structural and luminescent properties of $0.5SnO–24.5SrO–75B_2O_3$ (SSB) glasses prepared under different preparation conditions. The X-ray-induced luminescences, such as scintillation, thermally stimulated luminescence, and optically stimulated luminescence, of the SSB glasses are affected by the cooling process with different rates of change. For the present SSB glasses, we have found that the rapid cooling process is effective for attaining high luminescent intensities in all measurements.

1. Introduction

Glass is a metastable solid-state material obtained from the supercooled liquid state.[1–6] The structure and physical properties of the glass, therefore, depend on the preparation process. The most important point during the preparation process is a thermodynamically structural stabilization of the supercooled liquid, i.e., the crystallization of glass, above the glass transition temperature T_g. If the nominal chemical composition of glass is equal to the corresponding crystal, such structural stabilization is often observed even in the as-prepared glass prepared by rapid quenching. Structural ordering affects many parameters, such as the phonon vibration, energy propagation, and thermal stability of glass. Therefore, it is important to examine the glass structure for various applications.

In the case of phosphor application with doped activators, the local coordination states of the activators in glass are important for the improvement of performance, although the quantification of the glass network is difficult. Since glass has wide ranges of chemical compositions and metastable structures including several defects, it will have an advantage when phosphors exhibiting different responses in the same matrix are considered. Among several activators, we have selected ns^2-type cations ($n \geq 4$)[7–10] for the evaluation of local structural change. Because of the electron in the outermost shell in both the ground (ns^2) and excited states (ns^1np^1), the emission

*Corresponding author: e-mail: hirokazu.masai@aist.go.jp
http://dx.doi.org/10.18494/SAM.2017.1618

of ns^2-type cations is strongly affected by the local coordination state. These cations can exhibit high photoluminescence (PL) intensity because of parity-allowed transitions.[11–16] We have recently reported on the PL properties of xSnO–(25−x)SrO–75B_2O_3 glass,[15,16] a stoichiometric composition of a Sn-doped SrB_6O_{10} crystal.[17] In the case of 0.5SnO–24.5SrO–75B_2O_3 (SSB) glasses prepared at different cooling temperatures, the formation of a more dense glass network with slower cooling is observed as confirmed by the heat capacity, elastic modulus, ^{11}B NMR, first sharp diffraction peak of X-ray diffraction, and Boson peak results.[16] The optical absorption, PL, and Sn K-edge X-ray absorption fine structure data strongly suggest that the aggregation of Sn^{2+} results from the slow cooling of the melt, and that the PL properties of Sn^{2+} can be affected by the ordering of the transient state of supercooled liquid.[16]

On the other hand, we have also focused on the radioluminescence (RL: by X-ray or charged-particle excitation) of glass.[18–22] Since energy transfer from the host matrix to the activators is inherently contained in RL processes, especially in storage-type luminescence, the behavior of RL will be different from that of PL.[22,23] Therefore, it is important to examine the relationship between the RL of glass and the quenching process.

The aim of this work is to examine the relationship between the luminescent (PL and X-ray-induced RL) properties of Sn^{2+}-doped SrO–B_2O_3 glasses and quenching conditions. In addition to previous samples,[16] an additional glass was prepared for comparison. As RL properties, both nonstorage (scintillation) and storage [thermally stimulated luminescence (TSL) and optically stimulated luminescence (OSL)] luminescences were measured.

2. Experimental Procedure

2.1 Preparation of SnO-doped strontium borate glasses

The chemical composition of the present glasses was SSB (in mol%). A mixture of SnO, SrO, and B_2O_3 was melted in an electric furnace using a Pt crucible. Melting was performed at 1373 K for 20 min in ambient atmosphere, and the batch was about 9 g. To prepare the SSB glasses under different cooling conditions, three samples were prepared by pouring the glass melt onto a Pt plate in an electric furnace at temperatures of 373, 573, and 773 K. Considering the T_g (887 K) of the SSB glass prepared by a conventional melt quenching method, these annealing temperatures were selected. After pouring the glass melt, the glass samples were maintained at elevated temperatures for 1 h. On the other hand, one SSB glass was prepared by a conventional melt-quenching method in which the glass melt was quenched on a stainless steel plate maintained at room temperature (300 K). For several measurements, the glass samples were cut (~10 × 10 × 1 mm^3) and polished with aqueous diamond slurry.

2.2 Analysis methods

The experimental details of PL, photoluminescence excitation (PLE), density, and refractive index are shown in the previous paper.[16] The ^{11}B magic angle spinning (MAS) nuclear magnetic resonance (NMR) spectra of the glasses were obtained by using a JEOL DELTA 600 spectrometer. The chemical shift of ^{11}B MAS spectra was referenced using a 1 M H_3BO_3 aqueous solution at 19.6 ppm. To estimate the population and NMR parameters of boron species, spectral deconvolution was performed using the DmFit 2002 program with a "Q-mas 1/2" model[24] by considering

that the chemical shift of ^{11}B was mainly affected by its first coordination number, i.e., three-coordinated boron $BO_{3/2}$ and four-coordinated boron $BO_{4/2}$. The longitudinal elastic modulus c_{11} was calculated using the equation $c_{11} = \rho V_L^2$, where ρ is the density, and V_L is the longitudinal sound velocity. V_L was calculated using the equation $V_L = v_B\lambda/2n_{532}$, where v_B, λ, and n_{532} are the Brillouin shift, the wavelength of incident light (= 532 nm), and the refractive index at 532 nm, respectively. The details of the Brillouin scattering measurement are also shown in a previous paper.[16]

X-ray scintillation spectra at room temperature were observed using a monochromator equipped with a charge-coupled device (CCD, Andor). The irradiated dose was calibrated using an ionization chamber. The details are shown in a previous paper.[25] OSL spectra were recorded using Quantaurus-Tau (Hamamatsu Photonics) and the stimulation wavelength was 1.97 eV. TSL glow curves were recorded using TL-2000 (Nano Gray) with a heating rate of 1 K/s.

3. Results and Discussion

3.1 Structure of the SSB glasses

The obtained SSB glasses were transparent, and no diffraction peak due to crystallization was observed. First, we examined the effect of the quenching temperature on the structure of the SSB glasses. Figure 1(a) shows the ^{11}B MAS NMR spectra of the SSB glasses quenching at 300, 373, 573, and 773 K. As shown in Fig. 1(a), boron units can be classified into two species by the first neighborhood oxygens: four-coordinated boron $BO_{4/2}$ (located at 0 ppm) and three-coordinated

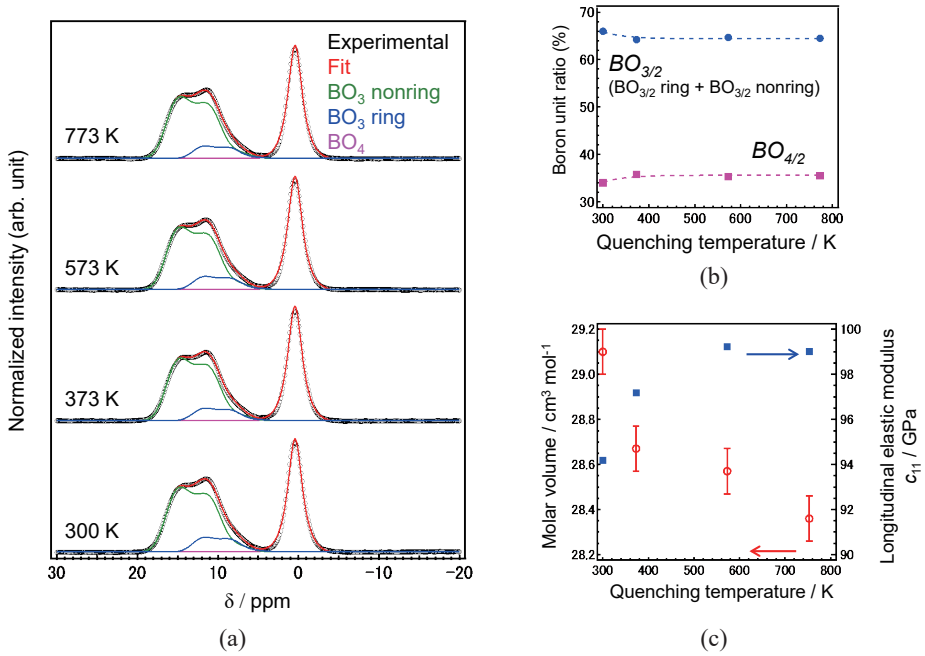

Fig. 1. (Color online) Structural and physical analyses of the SSB glasses. (a) ^{11}B MAS NMR spectra of the SSB glasses prepared at different quenching temperatures. (b) Boron unit ratio of the SSB glasses as a function of quenching temperature. (c) Molar volume and longitudinal elastic modulus of the SSB glasses as a function of quenching temperature.

boron $BO_{3/2}$ (other nonsymmetric peaks),[26–29] where the three-coordinated boron species consist of ring and nonring $BO_{3/2}$ structures. Figure 2(b) shows the ratio of $BO_{3/2}$ to $BO_{4/2}$ in the SSB glasses as a function of the quenching temperature. It suggests that a larger number of $BO_{3/2}$ units exist in the glass produced by quenching at a low cooling temperature. In the case of the four-coordinated $BO_{4/2}$ unit, a counter cation is required to compensate for the excess negative charge.[30] It is, therefore, expected that packing density will increase with $BO_{4/2}$ fraction. To confirm this expectation, the molar volume and the longitudinal elastic modulus c_{11} were measured. Figure 1(c) shows the molar volume and c_{11} of the SSB glasses as functions of the quenching temperature. c_{11} was calculated by using the equation $c_{11}=\rho \cdot v_L^2$, where v_L is the longitudinal sound velocity. With increasing quenching temperature, the molar volume decreases, whereas the elastic modulus increases. In the case of conventionally annealed SSB glass, the values of c_{11} and molar volume were 102 GPa and 28.2 $cm^3 \cdot mol^{-1}$, respectively. Compared with the conventional values, we can understand that a loose glass network was formed by the present preparation method. If we can use the technical word "fictive temperature", the fictive temperatures of these SSB glasses will be higher than that of the conventional one. These results are consistent with our expectation, and this clearly demonstrates that the glass structure changes depending on the preparation conditions.

3.2 PL properties of the SSB glasses

Next, we focused on the PL properties of doped Sn^{2+} centers. Figure 2(a) shows the PL and PLE spectra of the SSB glasses prepared under different quenching conditions. We confirmed that spectral shape changes depending on the cooling conditions. The spectral change is also observed in the PL-PLE contour plots of the SSB glasses shown in Fig. 2(b). Both the spectral shape and the emission intensity change, and the intensity decreases with increasing quenching temperature, i.e., slower cooling. Considering the densification of the glass network, it is expected that Sn^{2+} centers will aggregate to reduce the intensity. As discussed in the previous paper, the change in the local coordination state of Sn^{2+} centers was observed by Sn K-edge X-ray absorption fine structure (XAFS)

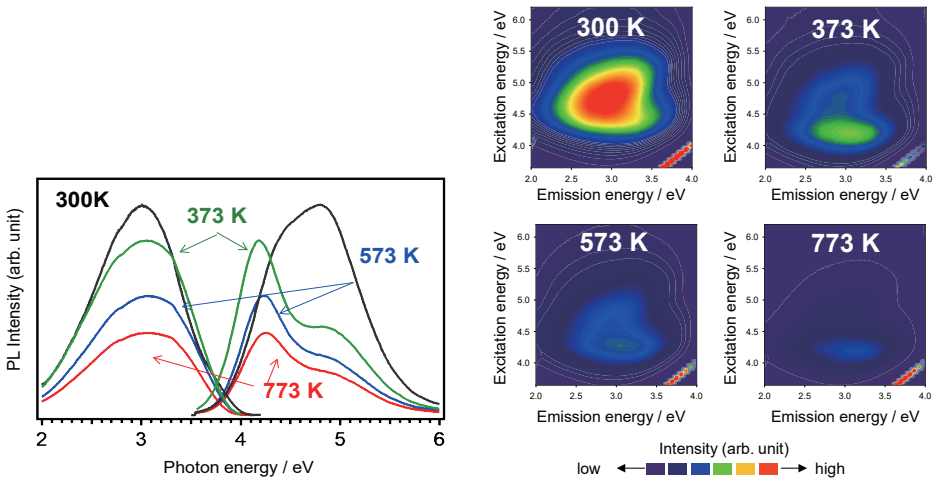

(a) (b)

Fig. 2. (Color online) PL of Sn^{2+} centers depending on the cooling conditions. (a) PL and PLE spectra of the SSB glasses prepared at different quenching temperatures: rapid quenching at 300 K and quenching at 373, 573, and 773 K. (b) PL-PLE contour plots of the SSB glasses.

analysis.[16] Although the oxidation of Sn^{2+} might be induced at 773 K, no apparent change was observed in the Sn K-edge X-ray absorption near edge structure (XANES) spectra. Since Sn^{2+} species have lone-pair electrons that hold free volume and exhibit a low melting behavior, it is expected that Sn^{2+} species will be excluded from the structural ordering of the glass to be aggregated. From the above analysis results, we conclude that the aggregation of Sn^{2+} cations occurs during the slower cooling of the glass melt along with the structural ordering of the host glass network.

3.3 X-ray-induced luminescence of the SSB glasses

Herein, we examined the X-ray-induced luminescent properties of the SSB glasses prepared at different quenching temperatures. Figure 3(a) shows the X-ray-induced scintillation spectra of the SSB glasses quenched at 300 K obtained at different irradiation doses. Photon energies at the emission peak of these glasses are almost constant independent of the quenching temperature and irradiation dose, which is also observed in PL spectra. Figure 3(b) shows the relationship between the scintillation intensities of the different SSB glasses and the irradiation doses of X-rays. These intensities are normalized using the volume of the samples. By comparing the scintillation intensities with the PL intensity, we observed that the dependence of scintillation intensity on quenching temperature is similar to that of PL, although no quantitative relationship between them is observed. It has been predicted that X-ray-induced scintillation is related to PL, because both luminescences are observed from the activators in the matrix. If the X-ray-induced scintillation efficiency η_{sci} is proportional to the PL quantum efficiency η_{PL}, the following relationships are obtained:[31–33]

$$\eta_{sci} = \eta_{PL} \times \alpha, \tag{1}$$

$$\alpha = \eta_{Xconv} \times \eta_{trans}, \tag{2}$$

where η_{Xconv} and η_{trans} are constants for conversion efficiency from X-rays to electron–hole pairs and energy transfer efficiency from the host to activators, respectively. If host matrixes exhibit different η_{Xconv} and η_{trans} values that are affected by several factors, such as the phonon vibration

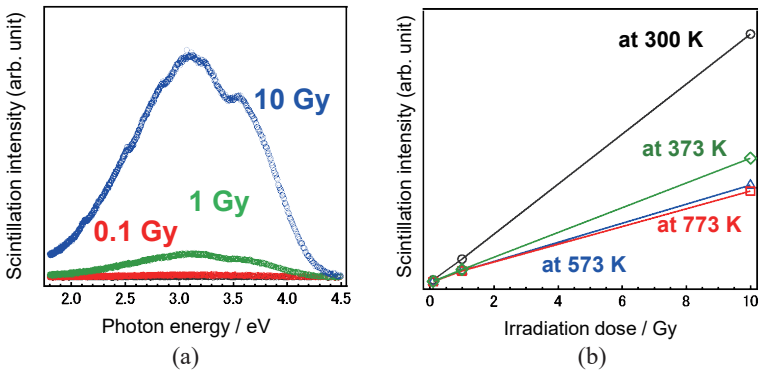

Fig. 3. (Color online) (a) X-ray-induced scintillation spectra of the SSB glasses prepared at 300 K. (b) Scintillation intensities of the SSB glasses prepared at different quenching temperatures as a function of irradiation dose.

and the concentration of activators, the intensity dependence of PL will be different from that of scintillation. The obtained results indicate that the α value of slowly cooled samples is lower than that of the quenched sample.

Figure 4(a) shows the TSL glow curves of the SSB glasses after 10 Gy irradiation. The SSB glasses prepared by slow cooling exhibit lower TSL intensities than the quenched one in the entire temperature range. TSL glow curves consist of at least two peaks, and the peak temperatures increase with the quenched temperature, i.e., slower cooling. This indicates that the trap depth is increased by the slow cooling process. Figure 4(b) shows the OSL spectra of the SSB glasses after 10 Gy irradiation. Similarly to the TSL intensity, the OSL intensity of the more slowly cooled sample is lower than that of the quenched one. Although the kind of trap that affects each storage luminesce may differ, the tendency against cooling rate is qualitatively similar. Since the densification of the host matrix is observed,[16] it is expected that this energy change will correlate with the stabilization of the host. On the other hand, there is an inverse correlation observed between scintillation and storage luminescence in several phosphors.[34] The obtained result demonstrates that this inverse relationship is not adoptable to the present case, mainly owing to the network stabilization.

Figure 5 shows the normalized emission peak area of the glasses as a function of quenching temperature. In all cases, the quenched sample exhibits a larger emission peak area than the slowly cooled samples. This is because of (1) the aggregation of Sn^{2+} centers to decrease the PL and

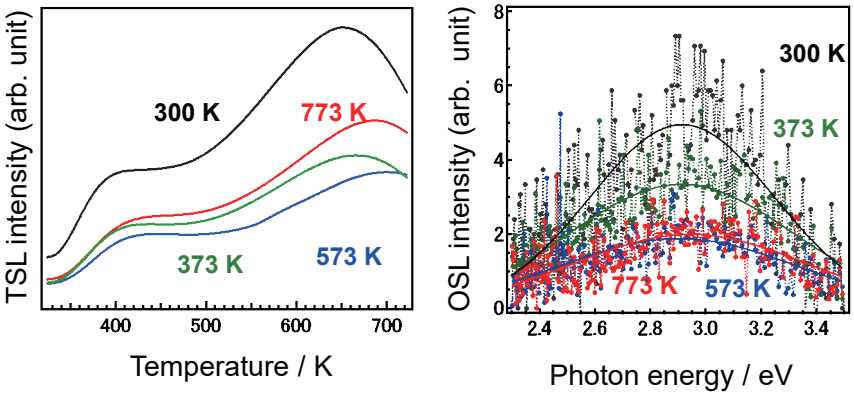

Fig. 4. (Color online) (a) TSL glow curves of the SSB glasses prepared at different quenching temperatures after 10 Gy irradiation. (b) OSL spectra of the SSB glasses prepared at different quenching temperatures after 10 Gy irradiation.

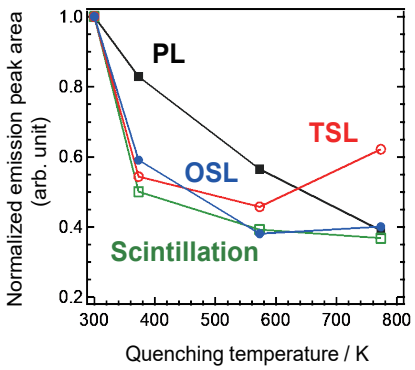

Fig. 5. (Color online) Normalized emission peak area of the glasses as a function of quenching temperature.

scintillation intensities, and (2) the stabilization of the host glass network to decrease the storage luminesce. Since this SSB glass has the stoichiometric chemical composition of the Sn-doped SrB_6O_{10} crystal,[16] it is expected that the stabilization of the host matrix, i.e., the ordering of the random network, will exclude impurities, such as dopants and defects. Therefore, we emphasized that the preparation process of glass materials affects both structural and physical properties.

4. Conclusions

We have demonstrated that both PL and X-ray-induced luminescence of Sn^{2+} centers in strontium borate glass, whose chemical composition is a stoichiometric composition of the corresponding crystal, are affected by the cooling conditions from the melt. Since the scintillation and storage luminescence of the quenched glass exhibit the highest efficiency, it is expected that the densification of the glass network will bring about the aggregation of activators and the decrease in the number of traps. Since the control of the local coordination state of the emission center will be important, it should be pointed out that both the chemical composition and the precise preparation control of glass are required for tailoring the designed properties.

Acknowledgments

This work was partially supported by the Grant-in-Aid for Young Scientists (A) 26709048, the Izumi Science and Technology Foundation, the Cooperative Research Project of the Research Institute of Electronics, Shizuoka University, and the Collaborative Research Program of the Institute for Chemical Research, Kyoto University (grant #2015-69 and #2016-83). The authors also thank Professor Masahide Takahashi (Osaka Prefecture University) for allowing them to use the prism coupler.

References

1 G. Adam and J. H. Gibbs: J. Chem. Phys. **43** (1965) 139.
2 C. A. Angell: J. Non-Cryst. Solids **131–133** (1991) 13.
3 C. A. Angell: Science **48** (1995) 279.
4 M. D. Ediger, C. A. Angell, and S. R. Nagel: J. Phys. Chem. **100** (1996) 13200.
5 V. Lubchenko and P. G. Wolynes: J. Chem. Phys. **121** (2004) 2852.
6 G. N. Greaves and S. Sen: Adv. Phys. **56** (2007) 1.
7 W. M. Yen, S. Shionoya, and H. Yamamoto, eds.: Phosphor Handbook, 2nd ed. (CRC Press, Boca Raton, USA, 2007).
8 J. A. Duffy and M. D. Ingram: J. Am. Chem. Soc. **93** (1971) 6448.
9 V. Dimitrov and S. Sakka: J. Appl. Phys. **79** (1996) 1736.
10 V. Dimitrov and T. Komatsu: J. Solid State Chem. **178** (2005) 831.
11 L. Skuja: J. Non-Cryst. Solids **149** (1992) 77.
12 R. Reisfeld, L. Boehm, and B. Barnett: J. Solid State Chem. **15** (1975) 140.
13 H. Masai, Y. Takahashi, T. Fujiwara, S. Matsumoto, and T. Yoko: Appl. Phys. Express **3** (2010) 082102.
14 H. Masai, T. Tanimoto, S. Okumura, K. Teramura, S. Matsumoto, T. Yanagida, Y. Tokuda, and T. Yoko: J. Mater. Chem. C **2** (2014) 2137.
15 H. Masai, Y. Yamada, Y. Suzuki, K. Teramura, Y. Kanemitsu, and T. Yoko: Sci. Rep. **3** (2013) 3541.
16 H. Masai, A. Koreeda, Y. Fujii, T. Ohkubo, and S. Kohara: Opt. Mater. Express **6** (2016) 1827.
17 M. Leskelä, T. Koskentalo, and G. Blasse: J. Solid State Chem. **59** (1985) 272.

18 H. Masai, T. Yanagida, Y. Fujimoto, M. Koshimizu, and T. Yoko: Appl. Phys. Lett. **101** (2012) 191906.
19 H. Masai, Y. Hino, T. Yanagida, Y. Fujimoto, K. Fukuda, and T. Yoko: J. Appl. Phys. **114** (2013) 083502.
20 H. Masai, Y. Suzuki, T. Yanagida, and K. Mibu: Bull. Chem. Soc. Jpn. **88** (2015) 1047.
21 H. Masai and T. Yanagida: Opt. Mater. Express **5** (2015) 1851.
22 H. Masai, Y. Ueda, T. Yanagida, G. Okada, and Y. Tokuda: Sens. Mater. **28** (2016) 871.
23 A. Torimoto, H. Masai, G. Okada, and T. Yanagida: Radiat. Meas. (in press). doi: https://doi.org/10.1016/j.radmeas.2017.01.017
24 D. Massiot, F. Fayon, M. Capron, I. King, S. Le Calvé, B. Alonso, J.-O. Durand, B. Bujoli, Z. Gan, and G. Hoatson: Magn. Reson. Chem. **40** (2001) 70.
25 T. Yanagida, Y. Fujimoto, T. Ito, K. Uchiyama, and K. Mori: Appl. Phys. Express **7** (2014) 062401.
26 J. Wu and J. F. Stebbins: J. Non-Cryst. Solids **356** (2010) 2097.
27 F. Angeli, O. Villain, S. Schuller, T. Charpentier, D. de Ligny, L. Bressel, and L. Wondraczek: Phys. Rev. B: Condens. Matter **85** (2012) 054110.
28 G. E. Jellison, Jr. and P. J. Bray: J. Non-Cryst. Solids **29** (1978) 187.
29 J. Zhong and P. J. Bray: J. Non-Cryst. Solids **111** (1989) 67.
30 J. Swenson, L. Börjesson, and W. S. Howells: Phys. Rev. B: Condens. Matter **52** (1995) 9310.
31 D. J. Robbins: J. Electrochem. Soc. **127** (1980) 2694.
32 A. Lempicki, A. J. Wojtowicz, and E. Berman: Nucl. Instrum. Methods Phys. Res., Sect. A **333** (1993) 304.
33 C. L. Melcher: Nucl. Instrum. Methods Phys. Res., Sect. A **537** (2005) 6.
34 T. Yanagida: J. Lumin. **169** (2016) 544.